INTRODUCTION TO PARAMETERIZATION OF PHYSICAL PROCESSES IN NUMERICAL MODELS[1]

R.A. Anthes
National Center for Atmospheric Research[2]
Boulder, Colorado, U.S.A.

Summary: This paper discusses the general problem of relating physical processes, such as turbulent fluxes of heat, moisture, and momentum, clouds and radiation, and changes of phase of water that are unresolvable by numerical weather prediction models to the parameters resolved and predicted by the model (a process termed parameterization). Evidence of the importance of these subgrid-scale processes to circulations ranging from the mesoscale to global scale and on time scales from less than a day to several weeks is presented.

1. INTRODUCTION

Numerical weather prediction models are limited in their accuracy by three sources of error: (1) truncation errors associated with the replacement of the continuous differential equations governing nonlinear fluid motion by approximations (e.g., finite differences or truncated spectral representations), (2) errors in the initial conditions of the atmospheric variables predicted by the model, and (3) errors in the approximations of complex physical processes such as radiation, condensation and evaporation, mixing of heat, moisture and momentum, and frictional dissipation.

---

[1]Paper presented at 1985 ECMWF Seminar "Physical Parameterizations for Numerical Models," Shinfield Park, Reading, United Kingdom, 9-13 September 1985.

[2]The National Center for Atmospheric Research is sponsored by the National Science Foundation.

It is of great theoretical and practical interest to determine the relative contribution to the total forecast error by each of the three classes of error. Such estimates are difficult to establish quantitatively. Wiin-Nielsen (1976) presents results from an analysis made by A. Robert based on an error budget over the relatively data-rich region of North America. Given the total error as 100%, he estimated the contribution due to various sources of error (Table 1).

Table 1. Contribution to total error in numerical weather prediction model for short-range forecasts (approximately two days) (Wiin-Nielsen, 1976).

Total Truncation Error (Horizontal 38%, vertical 9%, temporal 1%)	48%
Initial Conditions	18%
Physics	34%
Total	100%

The error estimates of Table 1 were conducted in the early 1970s with a five-level model with 381-km horizontal resolution which used second-order finite differences. Since then, advances in computing technology and numerical techniques have made it possible to run high-resolution models (15 layers with approximately 150-km horizontal resolution) with more accurate numerical approximations, so that the first source of error has undoubtedly been greatly reduced. The second two sources of error have yielded more slowly to improvements, and now may be identified as the major sources of errors in forecasts of up to several weeks. The purpose of this year's ECMWF Seminar Series is to review developments in the representation of physical processes in numerical models over the past decade.

The physical components of modern numerical weather prediction models include the modeling of energy sources and sinks associated with fluxes of heat, moisture, and momentum at the earth's surface, in the planetary boundary layer, and occasionally the free atmosphere. In the free atmosphere, these vertical fluxes may be associated with deep moist convection, vertically propagating gravity waves induced by flow over irregular surfaces (orographic effects), or instabilities which develop from large-scale processes (such as Kelvin-Helmholtz instabilities).

Other important physical processes include radiation and changes of phase of water in clouds of all types and scales. All of the above physical processes are highly interactive and are associated with scales of motion much smaller than those resolvable by models. For example, clouds involve scales of motion ranging from microphysical processes (10^{-8} m) to the global scale 10^{7} m, a range of more than 15 orders of magnitude in spatial scale (Fig. 1). The effect of physical processes such as clouds and radiation on the scales resolved by the model thus depend strongly on "subgrid-scale" processes. Relating the cumulative effects of these subgrid-scale processes to the resolvable scales of motion is known as parameterization. A brief review of approaches to parameterizing various physical processes is presented in the following sections, with some examples of the impact of these processes on model forecasts.

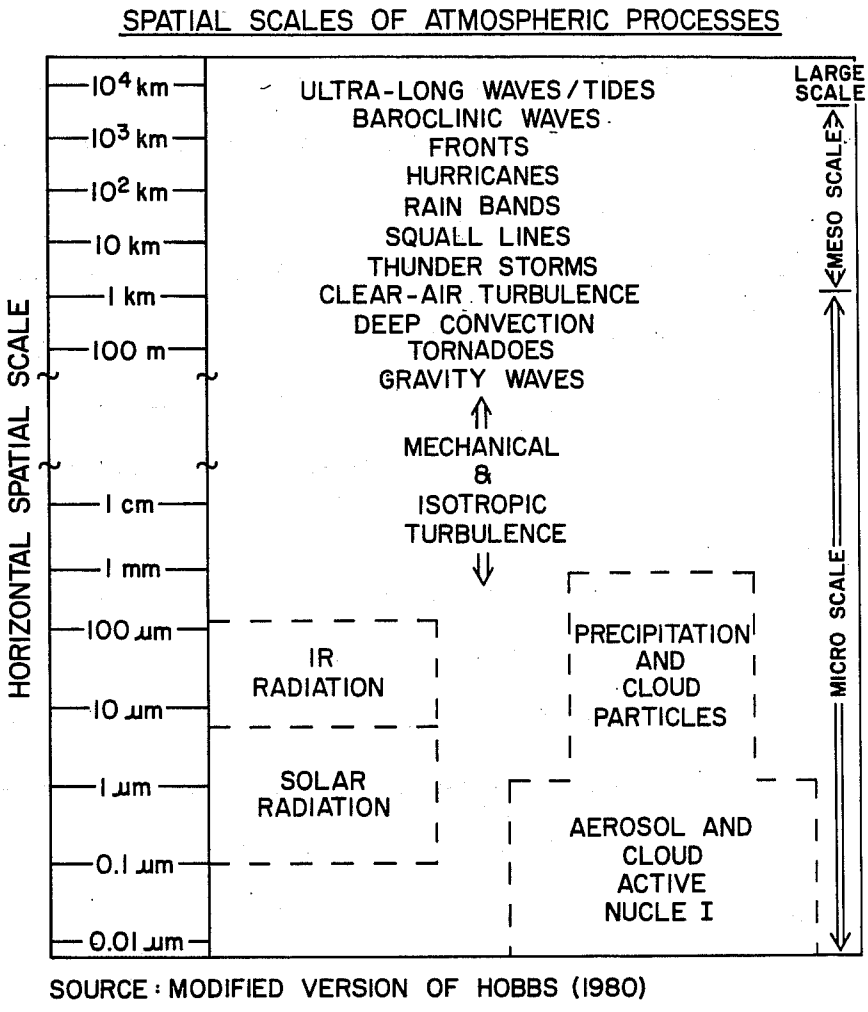

Fig. 1 Spatial scales of atmospheric processes (Hobbs and Deepak, 1981, modified by V. Ramanathan).

2. SURFACE PROCESSES

It is well-known that surface fluxes of heat, moisture, and momentum are important in determining the evolution of large-scale atmospheric circulations on long time scales (weeks to months). For example, the importance of surface heating and cooling in forcing the summer and winter monsoons over the Tibetan Plateau have been summarized by Gao et al. (1981). Tang and Reiter (1984) show a similar evolution of monsoon circulations over western North America. In contrast to their recognized importance on long time scales, surface energy fluxes have generally

been assumed to be relatively insignificant compared to large-scale atmospheric dynamics in determining atmospheric evolution, including precipitation, on time scales of a few days, except locally under large-scale conditions favorable for the development of mesoscale circulations such as sea breezes, mountain valley winds or other topographically induced mesoscale circulations. Most operational global and regional numerical weather prediction models have, therefore, utilized rather simple surface and planetary boundary-layer physics, and many ignore completely the diurnal radiation cycle.

There is abundant observational evidence to indicate the importance of diurnal variations in heating and cooling at the surface in generating significant diurnal variations in wind, divergence and vorticity, pressure, and precipitation patterns on all scales of motion, including the synoptic scale. Over 30 years ago, Bleeker and André (1951) explained the observed nocturnal maximum in thunderstorm frequency over the central United States as a result of "cooling and heating processes during the night and day (which) set up a large-scale circulation system east of the Rocky Mountains." More recently, Reiter and Tang (1984) showed that diurnal variations in heating and cooling over the high mountains of the western United States during the summer produced a heat low centered over Colorado, Wyoming, and Nevada during the day and an anticyclone during the night. Surface winds on a horizontal space scale of several thousand kilometers responded to this diurnal oscillation in pressure, which had an amplitude of 2-4 mb (much larger than the amplitude of the semi-diurnal pressure wave associated with atmospheric tides). The divergence associated with this large-scale circulation is apparently associated with the pronounced early afternoon maximum in

thunderstorm activity over the high terrain of the western United States (Wallace, 1975).

In contrast to the observational studies which indicate the importance of diurnal variations in the surface energy budget to large as well as small scales of motion, there have been few numerical studies to determine whether models can simulate the observed circulations. Benjamin and Carlson (1985) and Benjamin (1985) showed the importance of variations in cloud cover, elevation, and surface characteristics, including moisture availability, in generating meso-α (200-2,000 km) scale perturbations through differential heating at the surface for two cases of severe convective storm development over the central United States. Differences in sea-level pressure and boundary-layer winds between 12-h simulations with and without surface heat fluxes exceeded 4 mb and 7 m s^{-1} in some locations.

The above observational and numerical studies indicate that numerical predictions over time periods of a few days could be improved by inclusion of a diurnal cycle and better physical parameterization of surface and boundary-layer processes. Several parameterizations have been developed in recent years which treat the processes believed to be important in modulating the surface heat and moisture fluxes, including the effects due to varying roughness, albedo, moisture availability, vegetation, and surface heat capacity (Deardorff, 1978 and many others--see review by Pielke, 1984).

Zhang and Anthes (1982) tested a simple one-dimensional model of the moist PBL developed by A. Blackadar. The model consists of an atmospheric model coupled to a predictive model of ground potential

temperature (θ_g). The ground potential temperature is predicted through an energy budget equation

$$C_g \frac{\partial \theta_g}{\partial t} = R_n - H_m - H_s - E \ , \tag{1}$$

where C_g is the thermal capacity of the slab per unit area ($J\ m^{-2}{}^{\circ}C^{-1}$), H_m the heat flow into a substrate of constant temperature θ_m, H_s the heat flux into the atmosphere, and E the latent heat flux into the atmosphere. The thermal capacity C_g is related to the thermal conductivity λ of the soil layer and the heat capacity per unit volume C_s by

$$C_g = 0.95 \left(\frac{\lambda C_s}{2\omega}\right)^{1/2} \ , \tag{2}$$

where ω is the angular velocity of the earth. The sensible and latent heat fluxes are evaluated by expressions of the form

$$H_s = C_g F_1(u^*) \ (T_g - T_a) \ , \tag{3}$$

$$E = A_m F_2(u^*) \ (q_s \ (T_g) - q_a) \ , \tag{4}$$

where T_g is the ground temperature, q_s is the saturation specific humidity at T_g, T_a and q_a are atmospheric temperature and specific humidity at the lowest model level z_a (about 50 m), and F_1 and F_2 are functions of u^*, the friction velocity.

The parameter A_m is the "moisture availability," which is defined by Tanner and Pelton (1960) as the ratio of actual evaporation from a surface over the maximum possible evaporation, which would occur if the surface were saturated at the same temperature. Manabe et al. (1965) used this definition of A_m in a general circulation model.

The surface heat and moisture fluxes in the above model depend on four parameters that characterize the surface--moisture availability A_m, roughness length z_o (through its effect on u*), albedo A (through its effect on the net radiation R_n), and thermal capacity C_g. Of these four variables, Zhang and Anthes (1982) found the surface fluxes to be most sensitive to variations in A_m (Fig. 2). As A_m increased from 0

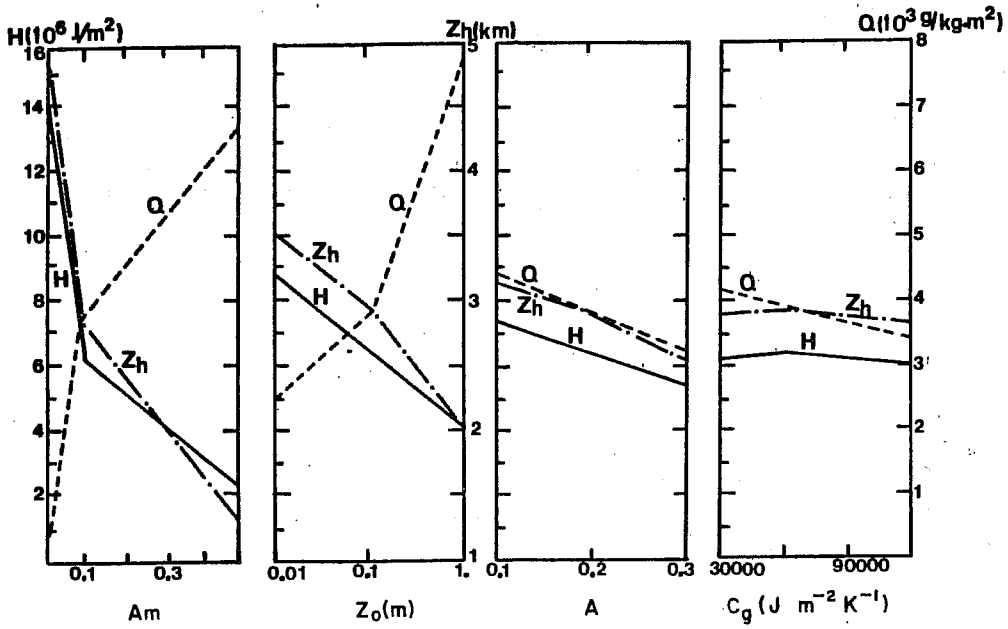

Fig. 2 Vertical integrals of 12-h sensible heat flux H, water vapor flux Q, and height of PBL Z_h for three values of moisture availability A_m, roughness parameter z_o, albedo A, and thermal capacity C_g (Zhang and Anthes, 1982).

to 0.5, the daily sensible heat flux decreased from 16×10^6 J m^{-2} to 2.2×10^6 J m^{-2}; the latent heat flux (evaporation) increased from 0 to over 6.6×10^3 g kg^{-1} m^{-2}; and the maximum height of the inversion at the top of the PBL during the day decreased from over 5 km to less than 1 km. These results indicate that the moisture availability is an important surface parameter to be specified or predicted in a large-scale model.

While parameterizations of surface and PBL processes have been extensively tested in one-dimensional models and have produced seemingly realistic results in some three-dimensional meso-γ scale (2-20 km) models (Pielke, 1984), they have not been extensively evaluated in meso-α scale models and global models. To illustrate the importance of surface processes, I present results from two three-day simulations over North America. The production of perturbation circulations by land-sea contrasts and differences in elevation in this region are studied quantitatively with a limited-area model initialized with no motion and a temperature and moisture sounding typical of summertime conditions over the central United States. In the first simulation, the moisture availability is 0; in the second simulation it is set equal to 0.3 over all land areas.

2.1 Summary of model

The model is based on the one described by Anthes and Warner (1978). The vertical coordinate is $\sigma = (p - p_t)/(p_s - p_t)$, where p is pressure, p_s is surface pressure, and p_t is the constant pressure at the top of the model (100 mb). These two experiments utilize a bulk aerodynamic formulation of the planetary boundary layer (PBL) following Deardorff (1972). The ground temperature is predicted from the surface energy budget model described by Zhang and Anthes (1982) and summarized in the previous section. For these simulations, there are 11 σ-levels (0.0, 0.1, . . . 1.0) with equal spacing, which gives ten layers of equal thickness at which the temperature, moisture, and wind variables are defined. The horizontal grid contains 46 points in the north-south direction and 61 points in the east-west direction; the grid size is 160 km. The albedo over land is 0.2 and C_g is 1.3×10^5 J m^{-2} K^{-1}.

Short-wave radiation and long-wave radiation are considered in the surface energy budget but not in the free atmosphere. These radiative fluxes depend on the model-simulated cloud cover in a parameterization developed by Benjamin and Carlson (1985).

The cumulus parameterization and treatment of nonconvective precipitation follow methods developed by Kuo (1974) and Anthes (1977). In the convective parameterization, the total latent heat release is proportional to the vertically integrated moisture convergence; the vertical distribution of the convective heating is specified from a constant profile, as in Anthes et al. (1983).

2.2 Results

In the first experiment, the moisture availability is zero over the land. Fig. 3 shows the sea-level pressure and PBL winds after three days. Surface heating has produced low pressure over the continent and a large-scale flow of air from sea to land. Heating over the elevated terrain of the Rocky Mountains has produced a heat low over the mountains and a pronounced convergence of PBL flow. This low-pressure system and the associated cyclonic circulation are similar to the monsoon circulation appearing in the composite July analysis of Tang and Reiter (1984). The mountains of Mexico and Central America, because of their height and relatively narrow width, generate PBL winds of over 15 m s^{-1} (Fig. 3).

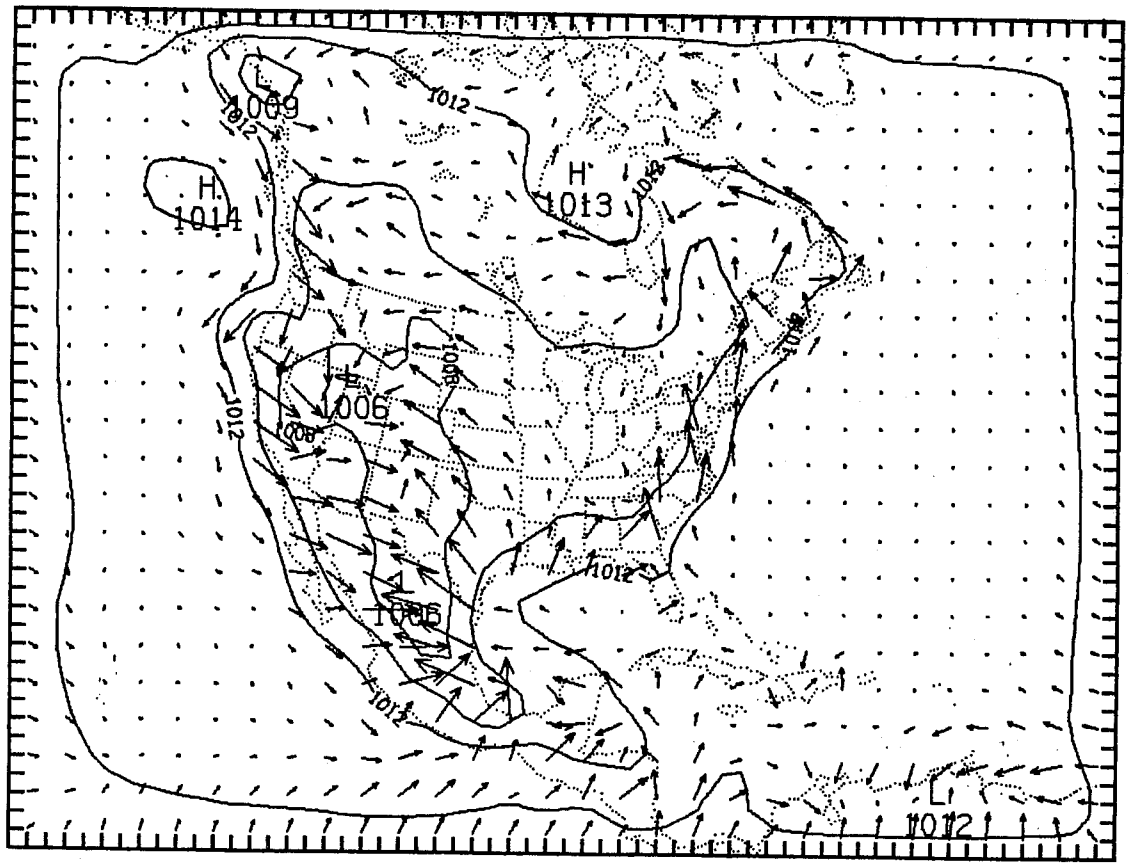

Fig. 3 Sea-level pressure (mb) and PBL (σ = 0.95) winds at 72 h of an integration initialized with zero winds and uniform temperature. The maximum wind is 15.5 m s^{-1}.

While the low-level circulation associated with the differential heating is characterized by cyclonic inflow with maximum convergence over the highest terrain, the upper tropospheric flow is dominated by divergent anticyclonic flow (not shown). The total circulation represents the North American monsoon circulation.

The convergence of low-level flow over regions of high terrain produces rainfall maxima over Colorado (0.10 cm), Mexico 2.40 cm, and the California Sierra Nevadas (0.36 cm) (not illustrated).

The second simulation is similar to the first except that the moisture availability over land is 0.3 rather than 0.0. The addition of evaporation over land causes significant differences at 72 h in the low-level temperature and moisture structure. The ground and PBL air temperatures over land are 3-4°C lower with evaporation, and the PBL mixing ratio is 7-8 g kg^{-1} higher. The cooler air over the land reduces the intensity of the heat-induced low-pressure region slightly, with a corresponding slight reduction in PBL winds. There is also a minor reduction in the strength of the upper-level branch of the monsoon circulation (not shown).

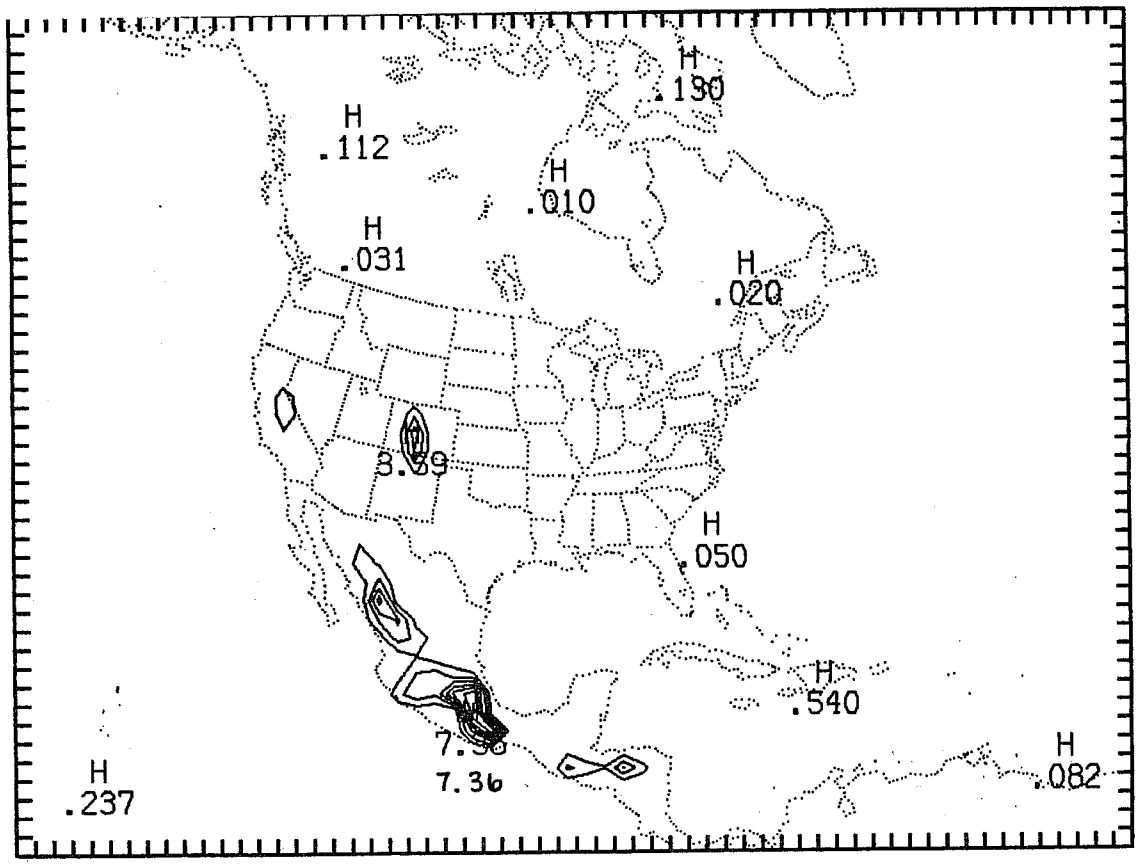

Fig. 4 Total precipitation (cm) after 72 h of an integration initialized with zero winds and uniform temperature. The contour interval is 1 cm.

Although the evaporation reduces the land-sea temperature contrasts and the strength of the monsoon circulation slightly, the rainfall increases considerably over the simulations with no evaporation. Fig. 4 shows the 72-h precipitation for M = 0.3. Rain maxima occur over the Caribbean Islands (0.54 cm), the Rockies of Colorado and New Mexico (3.59 cm), and Mexico (7.36 cm). The convective rainfall maximum over the high terrain of Colorado and New Mexico, with a sharp decrease toward the east, compares favorably with the average midday thunderstorm activity as revealed by the composite GOES satellite infrared imagery for August 1982 at 2100 GMT (Fig. 4 of Tang and Reiter, 1984).

3. SURFACE-LAYER AND PLANETARY BOUNDARY-LAYER PROCESSES

There are essentially two methods of parameterizing the surface layer (0-100 m) and the planetary boundary layer (PBL) in regional models. Most models use the well-known bulk aerodynamic method which treats the surface layer and PBL as a single layer and models the surface fluxes of heat, moisture, and momentum by exchange coefficients. The depth of the PBL may be fixed or vary in time (e.g., Deardorff, 1972), while the exchange coefficients may be constant or vary with roughness or static stability. The bulk-aerodynamic method is simple, computationally efficient, and has been reasonably successful.

In recent years, a number of high-resolution boundary-layer models have been developed and tested within a one-dimensional framework (Blackadar, 1979; Pielke, 1981). These models, though requiring more computer time (an additional five layers or so) provide for more generality than the bulk PBL models, for example, during the transition from well-mixed conditions to stratified nocturnal conditions in which strong vertical gradients of temperature, wind, and moisture often exist. Blackadar

presents additional arguments for the need for high-resolution PBL models. Considerable testing of various high-resolution PBL models in a one-dimensional framework is discussed in the literature (e.g., Burk, 1977; Chang, 1979; Yamada and Mellor, 1979).

Extensive studies of the role of surface fluxes and PBL processes in large-scale models have not been carried out, but a few research modeling studies indicate the importance of the PBL over periods as short as 0-24 h. For example, sea-level pressure forecasts have depended rather strongly on surface friction. Graystone (1962), Bushby (1968), Danard (1969), and Anthes and Keyser (1979) found differences of 5-20 mb in the minimum pressure of cyclones in 24-h forecasts with and without friction.

Other studies, using more sophisticated PBL models, have indicated the importance of surface fluxes on the temperature and moisture structure of the PBL. Yamagishi (1980) utilized a medium-resolution PBL model based on similarity theory and the level 2 (Mellor and Yamada, 1974) turbulent closure model in a forecast of a cold air outbreak over the Sea of Japan. His model simulated the observed heat and moisture fluxes and the height of the mixed layer reasonably well when accurate sea-surface temperatures were specified.

Miyakoda and Sirutis (1977) studied the response of a general circulation model to three different parameterizations. The schemes tested over a 30-day integration were (1) Mellor and Yamada's (1974) level 2.5 closure model, (2) a dry convective adjustment model (Manabe et al., 1965), and (3) a mixed-layer model developed by Randall and Arakawa. Both the level 2.5 closure model and the mixed-layer model produced more

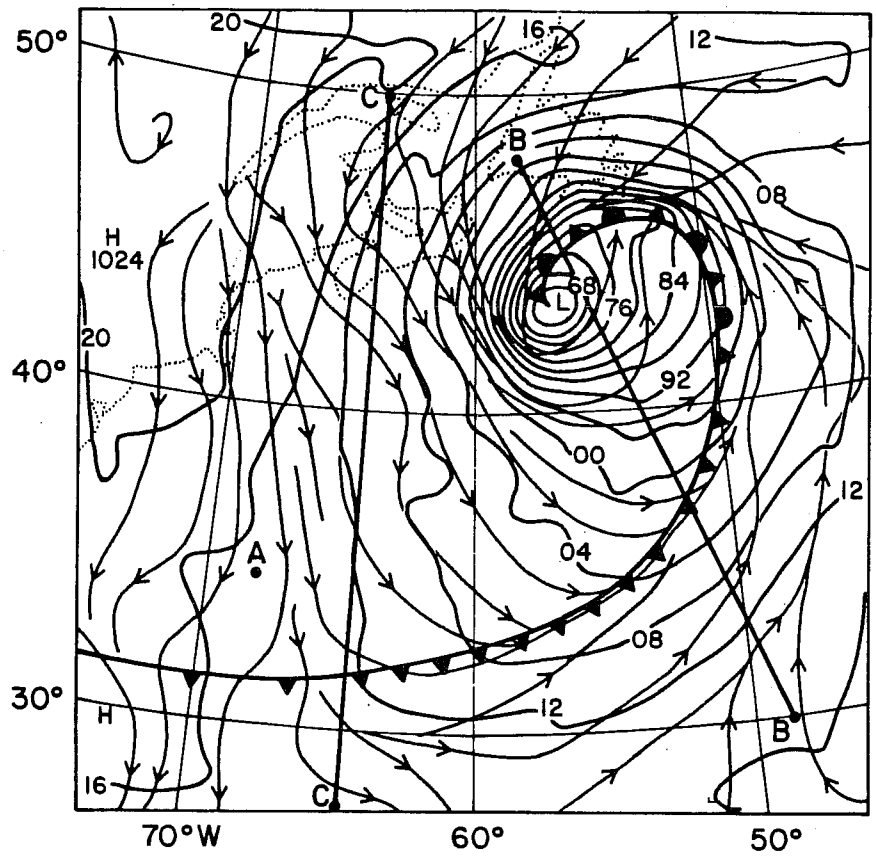

Fig. 5 24-h forecast for Exp. 7 (Anthes et al., 1983) of sea-level pressure (solid lines in mb) and streamlines at lowest level (σ = 0.999, z~8 m). The minimum pressure is 960 mb and the maximum wind speed is 50.2 m s^{-1} on the western side of the storm center. Fronts are located subjectively.

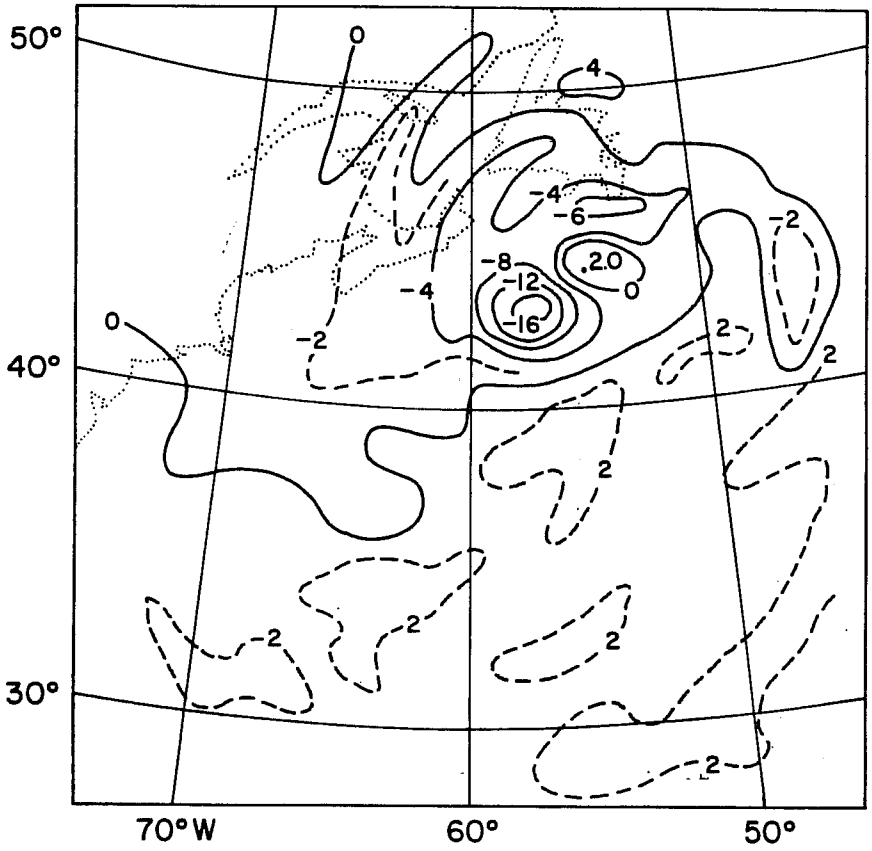

Fig. 6 Differences in surface pressure (contour interval 4 mb) between 24-h forecasts using medium-resolution PBL model (Exp. 7) and PBL model (Exp. 6) (Anthes, 1985).

realistic simulations than did the forecast with convective adjustment, which showed excessive cooling in the lowest 400 m.

In numerical simulations of a case of explosive marine cyclogenesis, Anthes (1985) compared simulations of the QE-II storm (an intense Atlantic storm of 9-10 September 1978, so named because it damaged the luxury liner Queen Elizabeth II) see Gyakum, 1983a,b, and Anthes et al., 1983) with two types of PBL parameterizations. One experiment (Exp. 6) used a bulk parameterization of the PBL following Deardorff (1972). The other experiment (Exp. 7) used the medium-vertical-resolution model of Zhang and Anthes (1982). Fig. 5 shows the 24-h forecast for Exp. 7 of sea-level pressure and streamlines at the lowest level of the model. Fig. 6 shows the difference in 24-h simulations of surface pressure between Exp. 7 (medium-resolution, explicit PBL model) and Exp. 6 (bulk PBL model). Although both experiments include surface energy fluxes, the simulation with the explicit PBL model shows a considerably more intense cyclone. As will be shown in subsequent analyses, this difference is probably caused by enhanced vertical transfer of energy away from the layer adjacent to the sea surface in Exp. 7 and a resulting increase of transfer of energy from the sea. The net effect is a greater energy input into the cyclone system.

Fig. 7 shows vertical cross section of differences in potential temperature and specific humidity between Exps. 7 and 6. The differences initiated by variations in the PBL formulation extend throughout the troposphere. The complex pattern reflects dynamical feedbacks associated with changes in intensity and location of the storm center. The significant differences are a warmer, drier central region of the storm and, in general, a thin layer of the drier air next to the surface. The drier layer allows for enhanced rates of evaporation in Exp. 7 and an

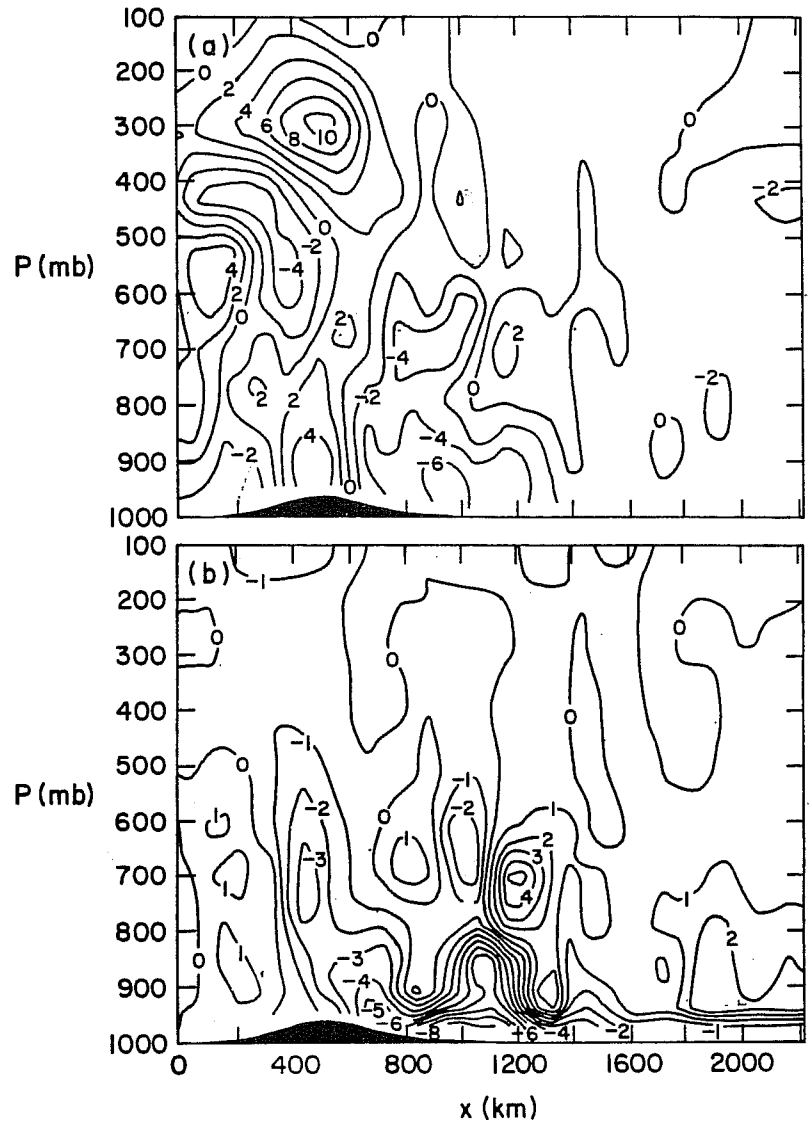

Fig. 7 Differences in potential temperature (a, contour interval 2 K) and specific humidity (b, contour interval 1 g kg^{-1}) along path B in Fig. 5 (through center of storm in Exp. 7) between 24-h forecasts using medium-resolution PBL model (Exp. 7) and bulk PBL model (Exp. 6) (Anthes, 1985).

increase in precipitation. The increased latent heating affects the structure above the PBL, resulting in a more intense storm.

Further insight into the differences in the vertical fluxes of heat and moisture associated with the two PBL models is provided by Fig. 8, which shows the vertical cross section along path C (Fig. 5) of differences in potential temperature and specific humidity. Exp. 7 shows a cooler, drier layer next to the ocean and a moister atmosphere above this layer. In the bulk-PBL model, the depth of the PBL is assumed to be constant with a top at a pressure of about 960 mb. The vertical fluxes of momentum and moisture are assumed to vanish at this level. However,

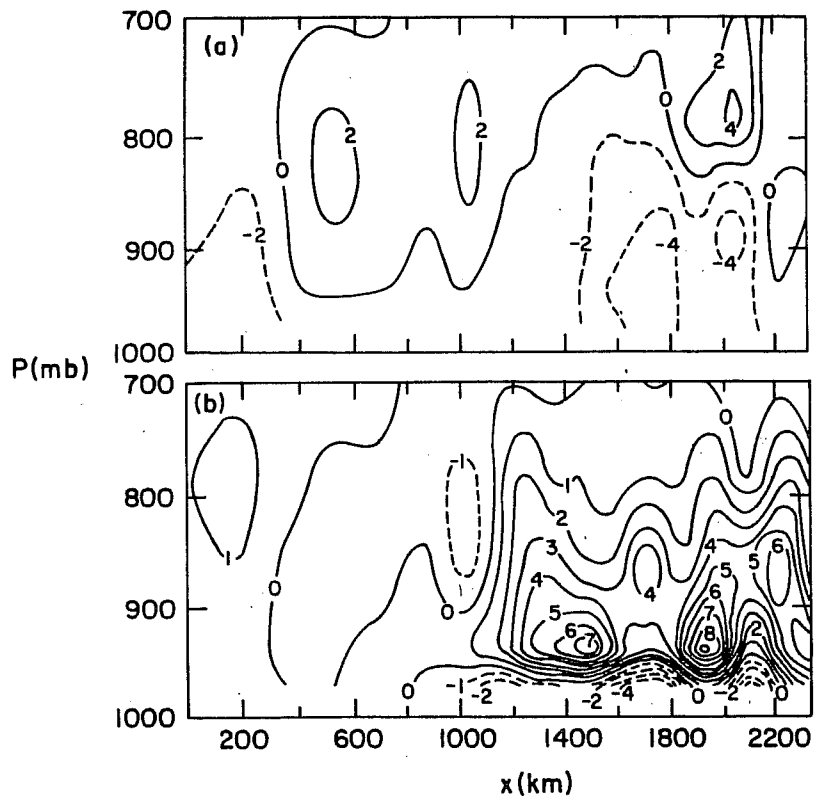

Fig. 8 Differences in potential temperature (a, contour interval 2 K) and specific humidity (b, contour interval 1 g kg^{-1}) along path C in Fig. 5 (normal to cold front) between 24-h forecasts using medium-resolution PBL model (Exp. 7) and bulk PBL model (Exp. 6) (Anthes, 1985).

with strong surface heating, heat may be transferred upward across this level by the dry convective adjustment mechanism in the model. In the explicit PBL formulation, however, the depth of the PBL varies and heat and moisture are both transferred upward throughout the PBL. In Exp. 7, the PBL becomes deeper than the constant value of Exp. 6. The vertical flux of moisture throughout this deeper layer dries the thin layer adjacent to the surface and moistens the upper layers. The drier surface layer permits more evaporation, so that there is a net increase of moisture in the lower troposphere (Fig. 8).

In summary, a formulation of the PBL processes based on explicit calculation of vertical fluxes within a PBL of variable depth gave a significantly different and more realistic lower tropospheric structure than did a bulk PBL formulation which assumed a constant PBL depth. Increased vertical transport of moisture out of the lowest model layer in the explicit PBL formulation permitted greater evaporation, a net increase of moisture in the lower troposphere, and a more intense storm.

3.1 Condensation and evaporation processes

The release of latent heat of condensation represents an important source of energy for synoptic-scale cyclones (Aubert, 1957; Danard, 1964; Tracton, 1973) and is also important in modifying the larger-scale environment. Observational studies (Ninomiya, 1971; Maddox et al., 1981; Fritsch and Maddox, 1981) have shown the development of anticyclonic perturbation flows in the upper troposphere over mesoscale regions of precipitation. The increasing baroclinicity often induces an upper-level jet streak north and west of the convective system.

Numerical models have successfully simulated the development of meso-scale convective systems and the effect of latent heat on the environmental flow. Chang et al. (1982) isolated the effect of latent heating on a 24-h forecast by subtracting a forecast without latent heating from a control forecast which obtained heating. They found that latent heating produced a perturbation circulation consisting of a warm upper-level anticyclone with maximum perturbation velocity of 30 m s^{-1} and a cold, lower tropospheric cyclonic perturbation with maximum velocity 20 m s^{-1}. A similar effect of latent heat has been found in other cases using other models with different parameterizations of convective heating. Anthes et al. (1982a) showed that latent heating induced a divergence anticyclonic wind perturbation near 300 mb with a maximum speed of more than 15 m s^{-1}. In the boundary layer, the latent heat generated a pressure decrease of more than 7 mb and a cyclonic circulation with perturbation wind speeds greater than 10 m s^{-1}. Similar results were obtained by Maddox et al. (1981) and Ninomiya and Tatsumi (1981).

Primitive-equation models have demonstrated the sensitivity of meso-α scale extratropical circulations to rather small changes in the specified vertical distribution of heating whenever substantial (greater than ~2 cm of rain per 12 h) precipitation is predicted. Anthes and Keyser (1979) showed an example of a 12-h forecast in which lowering the maximum in the specified vertical distribution of convective heating from 480 to 600 mb produced a cyclone with minimum pressure 11 mb lower. The greater proportion of heat released in the lower troposphere destabilizes the atmosphere and permits a much more rapid intensification. This interpretation is consistent with Sutcliffe's (1947) development theory, in which the greatest brake on a developing cyclone is the

adiabatic cooling associated with upward motion (Petterssen, 1956, p. 329). It is also consistent with Staley and Gall's (1977) study which showed that the wavelength of maximum growth in a baroclinically unstable environment shifts toward smaller wavelengths (~2,000 km) as the lower troposphere becomes less stable.

Numerical modeling simulations of explosive marine cyclogenesis (called "bombs" by Sanders and Gyakum (1980)) have shown considerable sensitivity to latent heating. Anthes et al. (1983) found differences in sea-level pressure of 17 mb in a 24-h forecast of the QE-II storm between experiments with and without latent heating. The simulation of the QE-II storm was also sensitive to the method of parameterizing the latent heating. In an experiment in which only grid-scale (resolvable) condensation and precipitation were allowed, a more intense storm (12 mb lower central pressure) was produced.

In recent research at NCAR of an intense cyclone over the eastern Pacific in November 1981, a simulation with a simplified version of the Anthes (1977) cumulus parameterization scheme produced a stronger storm than was forecast by the NMC Limited Fine-Mesh Model (LFM), but considerably weaker than observed (Fig. 9). However, when grid-scale condensation only was permitted, either through a prognostic equation for water vapor alone or with an explicit water cycle (prediction equations for cloud water and rain water in addition to water vapor), a much more intense storm was simulated (Fig. 9). These results are consistent with those found in the QE-II simulations and indicate that the vertical profiles of heating associated with the explicit schemes have maxima lower in the troposphere than the cumulus parameterization scheme.

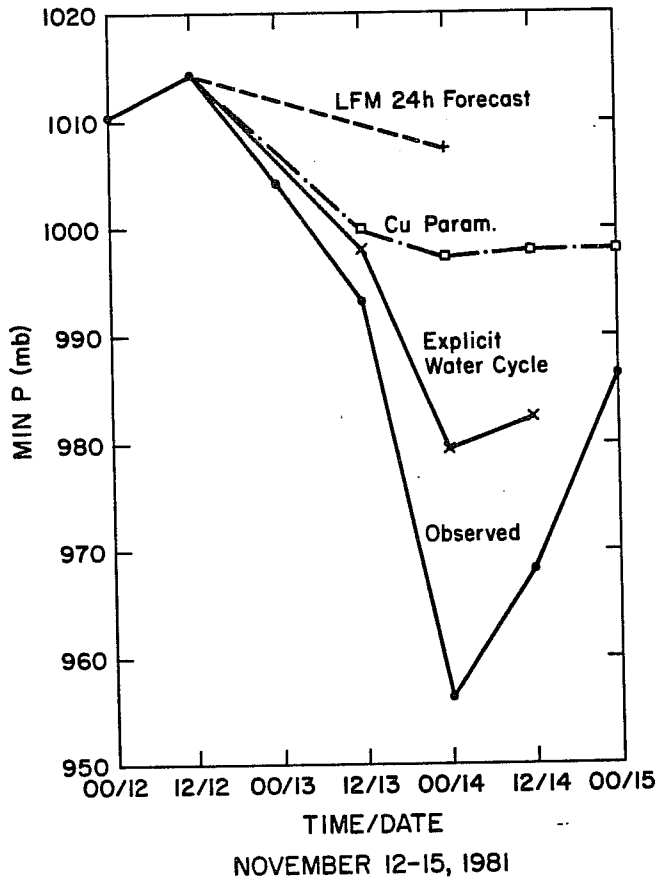

Fig. 9 Temporal variation of minimum pressure of observed and simulated Pacific storm of 12-15 November 1981.

3.2 Layered clouds and radiative effects

Because of energy transformations associated with changes of phase of water, and also because of their enormous effect on infrared and short-wave radiation, middle- and high-level clouds must be considered in large-scale numerical models. Even on time scales short as a day, there is evidence that clouds, through their effect on the surface energy budget, affect circulations in an important way (Benjamin and Carlson, 1985). Thus, it is necessary to model the major cloud effects as a function of the parameters predicted by the large-scale model. Until

recently, very simple parameterizations of nonprecipitating and precipitating middle- and high-level clouds have been used in global models. As summarized in Table 2, most GCMs assume the presence of nonconvective, stratiform middle and high clouds when the resolvable-scale relative humidity exceeds some critical value RH_c. For the ECMWF, GFDL, GLAS, UCLA, and GISS models, this value is 100%. For the NCAR model, RH_c is assumed to be 80% because of the possibility of having a fraction of the model's minimum resolvable scale covered by clouds when the average relative humidity is below 100%.

Table 2. Summary of nonconvective cloud parameterization in GCMs.

Model	Reference	Interactions with Radiation: Water Vapor	Interactions with Radiation: Clouds	Parameterization of Middle and High clouds	Resolvable-Scale Precipitation
ECMWF	Tiedtke *et al.* (1979)	I	I	S(RH_c = 100%)	E
GFDL	Holloway and Manabe (1977)	P	P	S(RH_c = 100%)	F
	Manabe *et al.* (1975)	I	P	S(RH_c = 100%)	F
GISS	Hansen *et al.* (1983)	I	I	S(RH_c = 100%)	E
GLAS	Somerville *et al.* (1974); Shukla and Sud (1981)	I	I	S(RH_c = 100%)	E
NCAR	Ramanathan *et al.* (1983)	I	I	S(RH_c = 80%)	F
UCLA	Arakawa and Lamb (1977)	?	?	S(RH_c = 100%)	E

P ≡ Prescribed as function of latitude, longitude, fixed in time
I ≡ Interactive
S = Clouds and resolvable-scale (stable) precipitation assumed to exist when grid-scale relative humidity exceeds prescribed value
F = Immediate fallout as precipitation
E = Evaporation into unsaturated lower layers until all layers saturated

Once clouds are diagnosed by the criterion RH > RH_c, the models treat the precipitation process and the interaction with radiation in different ways. The GFDL and NCAR models assume that the water vapor excess over RH_c falls to the ground immediately as precipitation (no evaporation), while the ECMWF, GLAS, UCLA, and GISS models allow evaporation in lower layers which are unsaturated. Only when the humidity of all lower layers equals RH_c does precipitation reach the ground.

Stephens (1984) reviews the radiation scheme of several GCMs (NCAR, GFDL, GISS, and GLAS). Early GCMs (e.g., Holloway and Manabe, 1971) did not allow the water vapor and clouds predicted or diagnosed by the model to interact with the radiation parameterization. Instead, water vapor and cloud effects on radiation were computed by assumed temporally constant fields of water vapor and clouds specified according to climatological fields. Recent GCMs relax this assumption by utilizing the model-predicted cloud and water vapor fields in the calculation of radiation effects. Shukla and Sud (1981) compared two climate simulations, one with prescribed clouds and another with interactive clouds. They found significant differences in the two climates; for example, the zonally asymmetric radiative heating associated with the fixed-cloud simulation produced greater generation of eddy available energy, more variance in the cyclone-scale transient waves, and large differences in the hydrologic cycle over the oceans.

Hansen et al. (1983) tested the sensitivity of the GISS GCM to variations in the treatment of clouds and their interaction with radiation processes. The sensitivity experiments are summarized in Table 3. In the control simulation, designated I-1, the fraction of the grid occupied by nonconvective clouds is computed under the assumption that the mixing ratio is constant in the grid volume but that temperature perturbations with a prescribed variance exist over the grid. The fraction of cloud cover is that fraction of the grid which is supersaturated owing to the temperature perturbations.

Table 3. Sensitivity of GISS GCM to variations in treatment of clouds (Hansen et al., 1983)

Exp.	Description
I-1	Control
I-35	No subgrid-scale temperature variance assumed in calculating fraction of grid covered by clouds
I-36	Large-scale rainfall calculated every 5 h rather than 1 h
I-37	Fixed annually averaged clouds from control simulation
I-38	Fixed annually and longitudinally averaged clouds from control simulation
I-39	Local temperature 0°C criterion for saturation over water or ice
I-40	Local temperature -40°C criterion for saturation over water or ice
I-41	Local temperature -65°C criterion for saturation over water or ice
I-42	Optical thickness of cirrus clouds reduced to $\tau = 1/3$
I-43	Optical thickness of other nonconvective clouds reformulated

In the first sensitivity experiment, I-35, the subgrid-scale temperature perturbation is eliminated in the calculation of the fraction of nonconvective cloud cover, i.e., grid-scale saturation is required for the presence of clouds and so the fraction of cloud cover is either 0 or 100%. This simulation was judged to be inferior to the control simulation in that unrealistically large low-level cloud cover was calculated over the oceans, particularly in the subtropical summer hemisphere. This result indicates that a parameterization that forces the extreme conditions of either no cloud or total cloud cover over grid scales of order 4° latitude by 5° longitude is unrealistic.

In Exp. I-36, the frequency for calculating the large-scale precipitation was decreased from every hour to 5 h. This allowed the relative humidity on the resolvable scale to build up to greater values before being reduced by precipitation and resulted in an increase in global

cloud cover from a value of 40% to a more realistic value of 45%. Although this increase resulted in a climate closer to the observed, the result is somewhat disturbing because of the arbitrary nature of the frequency of computing the precipitation.

In sensitivity experiment I-37, the annual mean cloud cover produced by the control simulation was specified rather than allowing a time-dependent cloud cover to evolve. This experiment is different from the one studied by Shukla and Sud (1981), who used observed cloud cover rather than a mean cloud cover generated by their model. Even with a model-generated temporally averaged cloud cover that varied with latitude, longitude, and height, the climate of I-37 differed in important ways from the control. For example, in the Aleutian region, which has more clouds in winter than in summer, the use of annual mean clouds produced a statistially significant weakening of the Aleutian low in winter. The average cloud cover for the months of January-March decreased by 6.2% while the mean sea-level pressure increased by 8.9 mb in Exp. I-37 compared to the control.

In Exp. I-38, the cloud cover was specified not only as an annual average from the control simulation, but also the longitudinal average. Specification of a zonally uniform cloud cover reduced longitudinal heating differences and led to a large (25%) decrease in eddy kinetic energy in the low-latitude troposphere. These results are consistent with the results of Shukla and Sud (1981).

Exps. I-39, I-40, and I-41 test the sensitivity of the model to the temperature below which sublimation of vapor to ice is assumed rather than

condensation from vapor to water. In the control simulation, sublimation is assumed at all layers if the lowest layer is below 0°C, while condensation is assumed if the lowest layer is above 0°C. Exps. I-39, I-40, and I-41 use the local layer temperature to determine whether condensation or sublimation occurs, with threshold temperatures of 0°C, -40°C, and -65°C, respectively.

Because of the lower saturation vapor pressure over ice compared to water, saturation is easier with respect to ice, and Exp. I-39 showed an increase of high (300 mb) clouds compared to the control simulation. Decreasing the threshold temperature from 0°C to -40°C or -65°C leads to large regions of air supersaturated with respect to ice but undersaturated with respect to water, and a reduction of high clouds.

In the final two sensitivity experiments involving the treatment of clouds, the optical thickness τ of the clouds was varied. The changes in the formulation of τ had a relatively minor effect on the simulations, compared to the other sensitivity experiments. The main difference was a reduction by 5-10 W m^{-2} of the annual mean net radiation gain at the top of the atmosphere and the ground.

In summary, experiments with GCMs indicate the importance of interactive, time-dependent clouds in determining the model climate. The models are also sensitive to the method of calculating the fraction of cloud cover, but not as sensitive to specifiying the optical properties of the clouds.

4. SUMMARY

This introduction to parameterization of physical processes in numerical weather prediction models presented evidence that physical processes associated with energy transfers at the earth's surface, turbulent fluxes in the planetary boundary layer, cumulus convection and stratiform precipitation, and clouds and radiation play a major role in governing atmospheric behavior on time scales as short as a day and on spatial scales ranging from the mesoscale to the global scale. It can be argued that deficiencies in the present physical parameterizations are now the greatest source of model error on time scales from a day or so to several weeks. The following lectures in this seminar series will cover many of the new developments in parameterization.

5. REFERENCES

Anthes, R. A., 1977: A cumulus parameterization scheme utilizing a one-dimensional cloud model. Mon. Wea. Rev., 105, 270-286.

Anthes, R. A., 1985: Modeling sea-air energy fluxes and their effects on explosive marine cyclogenesis. Papers in Meteorological Research, The Meteorological Society of the Republic of China, Taipei, Tawian, in press.

Anthes, R. A., and D. Keyser, 1979: Tests of a fine-mesh model over Europe and the United States. Mon. Wea. Rev., 107, 963-984.

Anthes, R. A., and T. T. Warner, 1978: Development of hydrodynamic models suitable for air pollution and other mesometeorological studies. Mon. Wea. Rev., 106, 1045-1078.

Anthes, R. A., Y.-H. Kuo, S. G. Benjamin, and Y.-F. Li, 1982: The evolution of the mesoscale environment of severe local storms: Preliminary modeling results. Mon. Wea. Rev., 110, 1187-1213.

Anthes, R. A., Y.-H. Kuo, and J. R. Gyakum, 1983: Numerical simulations of a case of explosive marine cyclogenesis. Mon. Wea. Rev., 111, 1174-1188.

Arakawa, A., and V. R. Lamb, 1977: Computational design of the basic dynamical processes of the UCLA general circulation model. Meth. Comp. Phys., 17, 173-265.

Aubert, E. F., 1957: On the release of latent heat as a factor in large-scale atmospheric motions. J. Meteor., 14, 527-542.

Benjamin, S. G., 1985: Some effects of surface heating and topography on the regional severe storm environment Part II: 2-D idealized experiments. Mon. Wea. Rev., 113, accepted.

Benjamin, S. G., and T. N. Carlson, 1985: Some effects of surface heating and topography on the regional severe storm environment Part I: 3-D simulations. Mon. Wea. Rev., 113, accepted.

Blackadar, A. K., 1979: High resolution models of the planetary boundary layer. Advances in Environmental Science and Engineering, 1, No. 1, J. R. Pfafflin and E. N. Ziegler, Eds., Gordon and Breach Scientific Publishing, 50-85.

Bleeker, W., and M. J. André, 1951: On the diurnal variation of precipitation over central U.S.A., and its relation to large-scale orographic circulation systems. Quart. J. Roy. Meteor. Soc., 77, 260-271.

Burk, S. D., 1977: A moist boundary layer with a higher order turbulence closure model. J. Atmos. Sci., 34, 629-638.

Bushby, F., 1968: Further developments of a model for forecasting rain and weather. Proc. WMO/IUGG Symp. Numerical Weather Prediction, Tokyo, Tech. Rep. Japan Meteor. Agency, No. 67, II-75-II-84.

Chang, C. B., and D. J. Perkey, 1982: A numerical case study of the effects of latent heating on a developing wave cyclone. J. Atmos. Sci., 39, 1555-1570.

Chang, S. W., 1979: An efficient parameterization of convective and nonconvective planetary boundary layers for use in numerical models. J. Appl. Meteor., 18, 1205-1215.

Danard, M. B., 1964: On the influence of released latent heat on cyclone development. J. Appl. Meteor., 3, 27-37.

Danard, 1969: Numerical studies of effects of surface friction on large-scale atmospheric motions. Mon. Wea. Rev., 97, 835-844.

Deardorff, J. W., 1972: Parameterization of the planetary boundary layer for use in general circulation models. Mon. Wea. Rev., 100, 93-106.

Deardorff, J. W., 1978: Efficient prediction of ground surface temperature and moisture, with inclusion of a layer of vegetation. J. Geophys. Res., 83, 1889-1903.

Fritsch, J. M., and R. A. Maddox, 1981: Convectively driven mesoscale weather systems aloft. Part I: Observation. J. Appl. Meteor., 20, 9-19.

Gao, Y.-xi, M.-cang Tang, Si-wei Luo, Z.-bao Shen, and C. Li, 1981: Some aspects of recent research on the Qinghai-Xizang Plateau meteorology. Bull. Amer. Meteor. Soc., 62, 31-35.

Graystone, P., 1962: The introduction of topographic and frictional effects in a baroclinic model. Quart. J. Roy. Meteor. Soc., 88, 256-270.

Gyakum, J. R., 1983a: On the evolution of the QE II storm. I. Synoptic aspects. Mon. Wea. Rev., 111, 1137-1155.

Gyakum, J. R., 1983b: On the evolution of the QE II storm. II. Dynamic and thermodynamic structure. Mon. Wea. Rev., 111, 1156-1173.

Hansen, J., G. Russell, D. Rind, P. Stone, A. Lacis, S. Lebedeff, R. Ruedy, and L. Travis, 1983: Efficient three-dimensional global models for climate studies: Models I and II. Mon. Wea. Rev., 111, 609-662.

Hobbs, P. V., and A. Deepak, Editors, 1981: Clouds, Their Formation, Optical Properties, and Effects. Academic Press, New York.

Holloway, J. L., Jr., and S. Manabe, 1971: Simulation of climate by a global general circulation model. Mon. Wea. Rev., 79, 335-370.

Kuo, H. L., 1974: Further studies of the parameterization of the influence of cumulus convection on large-scale flow. J. Atmos. Sci., 31, 1232-1240.

Maddox, R. A., D. J. Perkey, and J. M. Fritsch, 1981: Evolution of upper tropospheric features during the development of a mesoscale convective complex. J. Atmos. Sci., 38, 1664-1674.

Manabe, S., K. Bryan, and M. J. Spelman, 1975: A global ocean-atmosphere climate model. Part I. The atmosphere circulation. J. Phys. Ocean., 5, 3-29.

Manabe, S., J. Smagorinsky, and R. F. Strickler, 1965: Simulated climatology of a general circulation model with a hydrological cycle. Mon. Wea. Rev., 93, 769-798.

Mellor, G. L., and T. Yamada, 1974: A hierarchy of turbulence closure models for planetary boundary layers. J. Atmos. Sci., 31, 1791-1806.

Miyakoda, K., and J. Sirutis, 1977: Comparative integration of global models with various parameterized processes of subgrid-scale vertical transports. Beitr. Phys. Atmos., 50, 445-487.

Ninomiya, K., 1971: Mesoscale modification of synoptical situations from thunderstorm development as revealed by ATS III and aerological data. J. Appl. Meteor., 10, 1102-1121.

Ninomiya, K., and Y. Tatsumi, 1981: Forecast experiment of long-lived subtropical cumulonimbus cluster with 6-level 77 km-mesh primitive equation model. J. Meteor. Soc. Japan, 59, 709-721.

Petterssen, S., 1956: Motion and motion systems. Weather Analysis and Forecasting, Vol. 1, McGraw-Hill, 428pp.

Pielke, R. A., 1981: Mesoscale numerical modeling. Advances in Geophysics, Vol. 23, 185-344.

Pielke, R. A., 1984: Mesoscale meteorological modeling. Academic Press, New York, 612pp.

Ramanathan, V., E. J. Pitcher, R. C. Malone, and M. L. Blackmon, 1983: The response of a spectral general circulation model to refinements in radiative processes. J. Atmos. Sci., 40, 605-630.

Reiter, E. R., and M. Tang, 1984: Plateau effects on diurnal circulation patterns. Mon. Wea. Rev., 112, 638-651.

Sanders, F., and J. R. Gyakum, 1980: Synoptic-dynamic climatology of the "Bomb." Mon. Wea. Rev., 108, 1589-1606.

Shukla, J., and Y. Sud, 1981: Effect of cloud-radiation feedback on the climate of a GCM. J. Atmos. Sci., 38, 2337-2353.

Somerville, R. C. J., P. H. Stone, M. Halem, J. E. Hansen, J. S. Hogan, L. M. Druyan, G. Russell, A. A. Lacis, W. J. Quirk, and J. Tennebaum, 1974: The GISS model of the global atmosphere. J. Atmos. Sci., 31, 84-117.

Staley, D. O., and R. L. Gall, 1977: On the wavelength of maximum baroclinic instability. J. Atmos. Sci., 34, 1679-1688.

Stephens, G. L., 1984: The parameterization of radiation for numerical weather prediction and climate models. Mon. Wea. Rev., 112, 826-867.

Sutcliffe, R. C., 1947: A contribution to the problem of development. Quart. J. Roy. Meteor. Soc., 73, 370-383.

Tang, M., and E. R. Reiter, 1984: Plateau monsoon of the Northern Hemisphere: A comparison between North America and Tibet. Mon. Wea. Rev., 112, 617-637.

Tanner, C. B., and W. G. Pelton, 1960: Potential evapotranspiration estimates by the approximate energy balance method of Penman. J. Geophys. Res., 65, 3391-3412.

Tiedtke, M., J.-F. Geleyn, A. Hollingsworth, and J.-F. Louis, 1979: E.C.M.W.F. Model-Parameterization of Sub-grid Scale Processes. European Centre for Medium Range Weather Forecasts Technical Report No. 10, E.C.M.W.F., Shinfield Park, Reading, Berkshire, England, 46 pp.

Tracton, M. S., 1973: The role of cumulus convection in the development of extratropical cyclones. Mon. Wea. Rev., 101, 573-593.

Wallace, J. M., 1975: Diurnal variations in precipitation and thunderstorm frequency over the conterminous United States. Mon. Wea. Rev., 103, 406-519.

Wiin-Nielsen, A., 1976: Atmospheric predictability on various scales. Naturwissenschaften, 63, 506-512.

Yamada, T., and G. L. Mellor, 1979: A numerical simulation of BOMEX data using a turbulence closure model coupled with ensemble cloud relations. Quart. J. Roy. Meteor. Soc., 105, 915-944.

Yamagishi, Y., 1980: Simulation of the airmass transformation using a numerical model with a detailed boundary layer parameterization. J. Meteor. Soc. Japan, 58, 357-377.

Zhang, D., and R. A. Anthes, 1982: A high-resolution model of the planetary-boundary-layer sensitivity tests and comparisons with SESAME-79 data. J. Appl. Meteor., 21, 1594-1609.